

# Determining Idle Running and Short-Circuit Operating Characteristics of an Asynchronous Traction Motor

Presură (Nicolae) Raluca-Cristina\*, Nicolae Marian-Ștefan\*, Enache Sorin\* and Vlad Ion\*

\*University of Craiova / Faculty of Electrical Engineering, Romania, raluca.presura92@gmail.com

**Abstract** – It is proposed the possibility to simulate the idle running and short-circuit characteristics of an asynchronous traction motor. Based on the results, the motor parameters can be determined. In the modern design of asynchronous motors, the simulation of these characteristics is required as a mandatory stage. On this basis, the electromagnetic stresses and the constructive solutions are finally established, so that the engine corresponds in operation. The tests are important, as they allow for a computation of the motor parameters. There still exists the possibility to simulate the stationary and dynamic modes, in order to determine the behavior of the motor while running. The comparisons between the simulated and the data provided in the motor datasheet proves that the occurring errors are under the 2.1 % level accepted as precision level. The correctness of the simulations performed is important in operation, because with the parameters and the results obtained we can anticipate the behavior of the machine in the dynamic or stationary modes. The operating, starting and speed characteristics of the asynchronous traction motor must meet the high demands imposed by the complex equipment used in modern transport vehicles. Concerns related to the development of new methods and procedures to optimize the construction of the asynchronous motors used in traction, to find new mathematical models for the correct simulation of the operating characteristics, are a permanent activity. The simulations and experimental tests were carried out considering a traction motor from a diesel electric locomotive.

**Cuvinte cheie:** motoare asincrone de tractiune feroviara, modelare, simulare.

**Keywords:** railway asynchronous traction motors, modelling, simulation.

## I. INTRODUCTION

In its evolution, the human society has developed the transport infrastructure for people and goods, making it an essential and permanent concern.

The development and progress of modern societies have been made and materialized through improvements, modernization or discoveries in the field of transport, considering all the known paths [1-3].

The evolution stage of a society depends on the means of conveyance, influencing the living standards of its members.

From a mechanical point of view, the traction motor is subjected to shocks and strokes caused by the unevenness of the track, it is exposed to various external influences such as: dust, rain, snow.

The functional connection between the main subsystems, driving, braking and mechanically, of the traction vehicles, is made through the axles or wheels, the mechanical transmission and the traction motor [4-6].

The realization of this functional connection is made by the group of physical elements represented by: the traction motor with its devices placed in the rolling apparatus, the mechanical transmission (the cylindrical traction gear) and the motor axle.

It is obvious that all these constitute a complex assembly, in which the parameters of the transmission itself, and the mechanical construction of the traction motor are mutually conditioned.

The electric traction motors are mounted on the rail vehicles and mechanically coupled to the axle by means of the gear wheel mechanism.

The limited space available, the important mechanical demands that arise due to the permanent and large amplitude variation of the load, make the transmission system a very important problem.

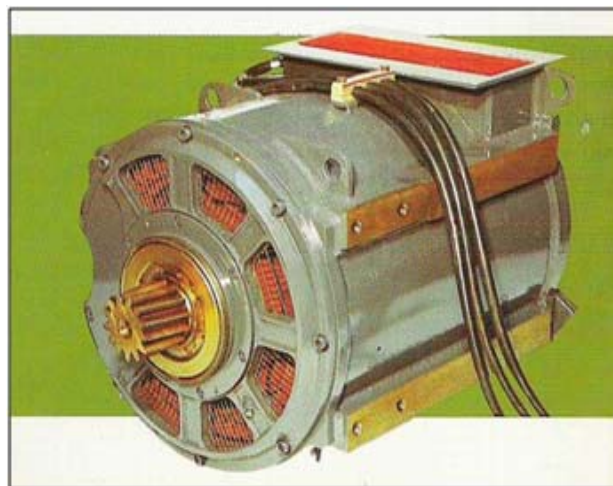


Fig. 1. Asynchronous motor used in railway traction.

By using asynchronous traction motors powered by static converters, the traction and electric braking performance are improved, while the maintenance costs are reduced.

Because the electric traction motor from Fig. 1 can have an efficiency even higher than 93%, the electric traction has some advantages provided by the regenerative braking, allowing for the conversion of the convoy's kinetic energy into electrical energy transferred to the

power line during the braking periods, stopping, or downhill.

When the regenerative braking is not possible, it can be automatically switched to rheostatic braking. Thus, the active energy of the motor running as a generator turns into heat wasted by the braking resistors.

The modern electric traction eliminates some of the existing drawbacks, by replacing the autonomous current inverters with autonomous PWM-controlled voltage source inverters.

The research is focused on finding new materials, the development of new topologies of electric motors, and also on the use of control and power electronics for increasing the effectiveness of the energy conversion.

In the modern electric traction [7-8] are used electronic converters with IGBTs, converters for ancillary services, control electronic equipment based on microcontrollers and microprocessors, LED lights, as in Fig. 2.

In Fig. 2 may be noticed: 1 – the electric locomotive, 2- buffers, 3 - driver's cab with all standard features, 4 – traction transformer, 5 – pantograph, 6 – brake system.

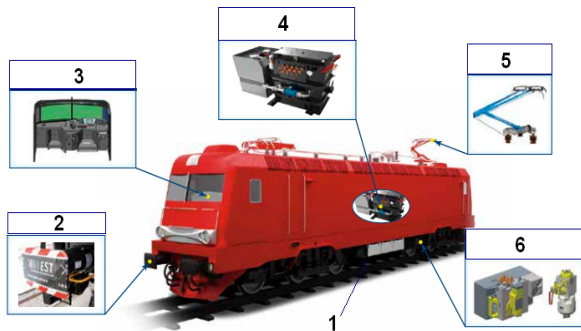


Fig. 2. Electric locomotive and main equipment.

The interest granted to the asynchronous motor transport vehicles came along with the development of the research.

The research is focused on finding new materials, the development of new topologies of electric motors, and also on the use of control and power electronics for increasing the effectiveness of the energy conversion.

The appropriateness of this work is provided by highlighting some aspects insufficiently treated in the areas of designing and dimensioning of asynchronous traction motors associated with large power static converters. The traction system is used for railway vehicles, the establishing of the parameters necessary in the analysis of the regenerative braking system being an important step.

Multiple and repeated simulations were carried out, and their quality highlights the motor's technical performances, thus responding to the requirements of the beneficiary.

## II. RESULTS OBTAINED THROUGH SIMULATION

Theoretical research and experimental tests were carried out for the traction motor from a diesel electric locomotive with a power of 2100 hp. This is an asynchronous three-phase traction motor with wound rotor, with the following parameters:

- rated values -  $P_N=260$  kW - rated power;  $U_N=1500$  V - rated voltage;  $I_{1N}=121.4$  A - rated current;  $n_1=1000$

rpm-synchronous speed;  $M_N=2537$  Nm - rated torque;  $s_N=2.1\%$  - rated slip;

-electric parameters  $R_s=0.247$   $\Omega$ ,  $R'_r=0.17$   $\Omega$ ,  $L_{s\sigma}=0.00255$  H,  $L'_{r\sigma}=0.001818$  H,  $L_{sh}=0.081$  H,  $J=2.791$  kgm<sup>2</sup>

-operating parameters:  $\cos\varphi=0.90$ ;  $\eta=0.916$ ;  $M_{max}=2.48 \cdot M$ ;

- imposed gauge dimensions:

$L_{max} < 580$  mm - maximum length;

$D_{max} < 795$  mm - maximum outer diameter.

### A. Mathematical model of mechanical characteristics

For an accurate simulation of the mechanical characteristics [9-12], the rotor and stator parameters affected by the repression and magnetic saturation are considered, the next steps being completed:

-the number of points necessary for representing the mechanical characteristics is set to  $N=800$ , while the variable  $i$  is initialized

$$i = 0, 1, 2, \dots, 2 \cdot N$$

-the slip is determined

$$s_i = -1 + \frac{i}{N}$$

-the speed is computed as:

$$n_i = n_1(1 - s_i),$$

while the slip in per unit (p.u.) values is:

$$nr_i = \frac{n_i}{n_1}$$

Thereby, a range is set for the slip,  $s \in [-1, +1]$ , and for the speed,  $n \in [0, 2 \cdot n_1]$ , respectively, in order to include the generator and asynchronous motor operating modes.

### B. The variation of the rotor winding parameters with the current repression in the rotor bar

-the reduced height of the conductor is calculated

$$\xi_i = h_b \sqrt{\frac{b_b}{b_{c2}} \cdot \frac{100 \cdot \mu_0 \pi f_1 |s_i|}{2\rho_{02}}}$$

$b_b$ ,  $h_b$  (mm) –dimensions of the rotor bar;  $b_{c2}$  (mm) – rotor slot width,  $\rho_{02}$  -bar resistivity (the bar is made of copper);

-the factor of resistance increase in the rotor slot area:

$$kr_i = \xi_i \frac{sh(2\xi_i) + \sin(2\xi_i)}{ch(2\xi_i) - \cos(2\xi_i)}$$

- the factor of reactance decrease in the rotor slot area:

$$kx_i = \frac{3}{2\xi_i} \frac{sh(2\xi_i) - \sin(2\xi_i)}{ch(2\xi_i) - \cos(2\xi_i)}$$

-the factor of resistance increase for the rotor bar:

$$Kr_i = kr_i \frac{l_{Fe}}{L_b} + \frac{L_b - l_{Fe}}{L_b}$$

$l_{Fe}/L_b$  - the iron length / the length of the rotor bar;  
 -the factor of reactance decrease in the rotor bar:

$$Kx_i = kx_i \frac{l_{Fe}}{L_b} + \frac{L_b - l_{Fe}}{L_b}$$

-the phase resistance considering the repression influence:

$$R2_i = Kr_i R_b + \frac{R_i}{2 \cdot \sin^2 \left( \frac{\pi p}{N_{c2}} \right)}$$

$R_b/R_i$  -bar resistance / resistance of the short-circuit ring;  
 $N_{c2}$  -number of rotor slots;

-the leakage permeance of the rotor slot, affected by the repression:

$$\lambda_{c2\xi} = \frac{h_{1r}}{3b_{c2}}$$

-the leakage permeance of the rotor slot, not affected by the repression:

$$\lambda_{c2h} = \frac{h_{1r} - h_b}{2b_{c2}} + \frac{h_{02}}{b_{02}}$$

$h_{02}/b_{02}$  - height and width of the rotor slot isthmus;

-the total permeance of the rotor slot considering the influence of the repression:

$$\Sigma \lambda_{2\xi_i} = Kx_i \lambda_{c2\xi} + \lambda_{c2h} + \lambda_{d2} + \lambda_{f2}$$

$\lambda_{d2}/\lambda_{f2}$  - front and differential, rotor leakage, specific permeances;

- the phase dispersion reactance of the rotor, considering the repression:

$$X_{2\xi_i} = X_2 \cdot \frac{\Sigma \lambda_{2\xi_i}}{\Sigma \lambda_2}$$

$X_2$  - dispersion phase reactance of the rotor, without considering the repression;

### C. Variation of the asynchronous motor parameters with the magnetic saturation

The parameters of the asynchronous motor dependent on the magnetic saturation are the leakage reactances corresponding to the stator and rotor, respectively. The effects of the magnetic saturation are obvious when the load current increases, exceeding the rated current, thus modifying the form of the mechanical characteristics. Therefore, an exact simulation of the mechanical characteristics is realized with the corrected parameters.

As such, the current curve throughout the startup in relative units  $i_p = f(s)$  is estimated to be a parabola having Os as the axis of symmetry (Fig. 3).

Under these circumstances, the following equation is needed:

$$s = a \cdot (i_p)^2 + b \cdot i_p + c$$

imposing that the points B( $s=1$ ,  $i_p=i_{pi}$ ) -for the start instant,  $H_0$  ( $s=0$ ,  $i_p=i_0$ ) -for the idle running and A( $s=s_N$ ,  $i_p=1$ ) -the operating point for the rated mode, be on the same parabola, thus resulting the coefficients:

$$a = \frac{\Delta_a}{\Delta}, \quad b = \frac{\Delta_b}{\Delta}, \quad c = \frac{\Delta_c}{\Delta}$$

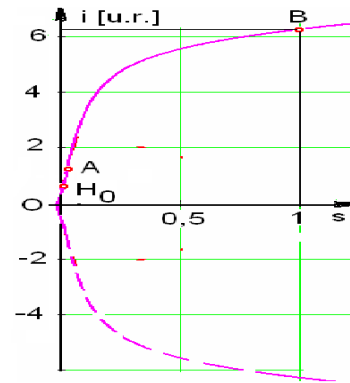


Fig. 3. The estimated current curve during motor startup.

$$\Delta_a = \begin{vmatrix} 1 & i_{pi} & 1 \\ 0 & i_0 & 1 \\ s_N & 1 & 1 \end{vmatrix}, \quad \Delta_b = \begin{vmatrix} i_{pi}^2 & 1 & 1 \\ i_0^2 & 0 & 1 \\ 1 & s_N & 1 \end{vmatrix}$$

$$\Delta_c = \begin{vmatrix} i_{pi}^2 & i_{pi} & 1 \\ i_0^2 & i_0 & 0 \\ 1 & 1 & s_N \end{vmatrix}, \quad \Delta = \begin{vmatrix} i_{pi}^2 & i_{pi} & 1 \\ i_0^2 & i_0 & 1 \\ 1 & 1 & 1 \end{vmatrix}$$

Solving the equation:

$$a \cdot (i_p)^2 + b \cdot i_p + c - s = 0,$$

with respect to the variable  $s$ , and the unknown variable  $i_{pi}$  and, considering only the positive side, is obtained:

$$i_{pi} = \frac{-b + \sqrt{b^2 - 4a(c - |s_i|)}}{2a},$$

-the variation of the permeability with the current during startup, due tot the saturation of the magnetic circuit, is provided by:

$$\mu_i = \frac{B_{dk}}{100 \cdot \mu_0 (H_{dk} + A \cdot i_{pi})}$$

$B_{dk}=2.04$  T - the critical value of the magnetic flux density;

$H_{dk}=300$  A/cm - the critical value of the magnetic field strength.

### E. The reactance of the stator winding considering the influence of the magnetic saturation

-the width of the stator slot isthmus when the magnetic saturation occurs:

$$b_{01s_i} = b_{01} + \frac{b_{d01}}{\mu_i}$$

$b_{01}/h_{01}$  – width / height of the stator slot isthmus;

$b_{d01}$  – the width of the tooth at the stator surface;

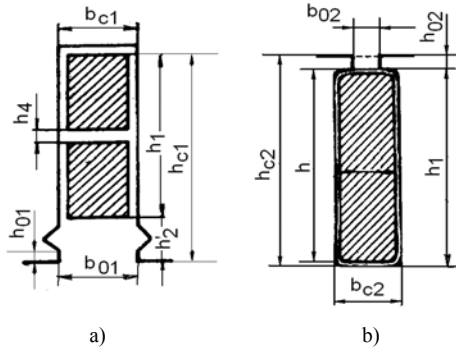


Fig. 3.4. a) rectangular stator slot open; b) rectangular stator slot semi-close.

-leakage permeance of the stator slot accounting for the saturation:

$$\lambda_{c1s_i} = \frac{h_{1s} - h_{4s}}{3b_{c1}} k_{\beta} + \frac{h_{2s}}{b_{01s_i}} k'_{\beta} + \frac{h_{4s}}{4b_{c1}}$$

$h_{1s}$ ,  $h_{2s}$ ,  $h_{4s}$  – constructive dimensions associated to the stator slot;

$k_{\beta}$ ,  $k'_{\beta}$  - factors depending on the stator winding step;

-total permeance of a stator phase, accounting for the saturation:

$$\Sigma\lambda_{1s_i} = \lambda_{c1s_i} + \lambda_{d1s} + \lambda_{f1}$$

$\lambda_{d1s}$ ,  $\lambda_{f1}$  – the saturation-specific and frontal stator differential permeance;

-the stator phase reactance, considering the saturation:

$$X_{1s_i} = X_1 \cdot \frac{\Sigma\lambda_{1s_i}}{\Sigma\lambda_1}$$

$X_1$  – the phase reactance of a stator winding, without considering the saturation.

#### F. The reactance of the rotor winding, considering the influence of the magnetic saturation

-width of the rotor slot isthmus when the magnetic saturation occurs:

$$b_{02r_i} = b_{02} + \frac{b_{d02}}{\mu_i}$$

$b_{02}/h_{02}$  – the width / height of the rotor slot isthmus;

$b_{d02}$  – tooth width at the rotor surface;

-the leakage permeance of the rotor slot, affected by the magnetic saturation:

$$\lambda_{c2hs_i} = \frac{h_{1r} - h_b}{2b_{c2}} + \frac{h_{02r}}{b_{02r_i}}$$

$h_{1r}$ ,  $h_b$  – constructive dimensions associated to the rotor slot;

-the total permeance of the rotor, considering the saturation:

$$\Sigma\lambda_{2s_i} = Kx_i\lambda_{c2\xi} + \lambda_{c2hs_i} + \lambda_{d2s} + \lambda_{f2}$$

$\lambda_{d2s}$ ,  $\lambda_{f2}$  – front and differential, rotor leakage, specific permeances;

-rotor phase reactance, influenced by the saturation:

$$X_{2s_i} = X_2 \cdot \frac{\Sigma\lambda_{2s_i}}{\Sigma\lambda_2}$$

$X_2$  – phase reactance of a rotor winding, without considering the saturation;

#### Rotor parameters reported to the stator

-the phase resistance / reactance reported to the stator:

$$R'_{2i} = k_{rap} R_{2i}$$

$$X'_{2s_i} = k_{rap} X_{2s_i}$$

- the saturation correction factor:

$$c_{1s} = 1 + \frac{X_{1s}}{X_{1m}}$$

#### G. Electromagnetic torque

$$M_i = \frac{m_1 p}{2\pi f_1} \cdot \frac{U_1'^2 \frac{R_{2i}}{s_i}}{\left(R_1 + c_{1s} \frac{R_{2i}}{s_i}\right)^2 + \left(X_{1s_i} + c_{1s} X_{2s_i}\right)^2}$$

- the electromagnetic torque computed for a different voltage and frequency results:

$$M'_i = \frac{m_1 p}{2\pi f_1'} \cdot \frac{U_1'^2 \frac{R_{2i}}{s_i}}{\left(R_1 + c_{1s} \frac{R_{2i}}{s_i}\right)^2 + \left(\frac{f_1'}{f_1}\right)^2 \left(X_{1s_i} + c_{1s} X_{2s_i}\right)^2}$$

where, e.g.  $f_1' = 1.5 \cdot f_1$  and  $U_1' = 1.5 \cdot U_1$

- the torque in per unit values is:

$$m_i = \frac{M_i}{M_N}$$

### III. RESULTS AND SIMULATIONS OF CHARACTERISTICS

With these quantities are drawn the mechanical characteristics. For obtaining the plots are used the following per unit (p.u.) values:

-  $n[r.u.] = n/n_1$  speed in p.u.;

- $m[r.u.] = M/M_N$  torque in p.u.;
- $i_1[r.u.] = I_1/I_{1N}$  current in p.u.;
- $r_2 = R_2/R_{20}$  rotor resistance in p.u.;
- $x_{1s} = X_{1s}/X_{10}$  stator reactance in p.u.;
- $x_{2s} = X_{2s}/X_{20}$  rotor reactance in p.u.;

Because during startup the frequency of the electromagnetic field is variable inside the rotor ( $f_2 = s \cdot f_1$ ), the resistance of the rotor winding is modified with the slip (Fig. 4.a) for the machine either running as a motor or as a generator.

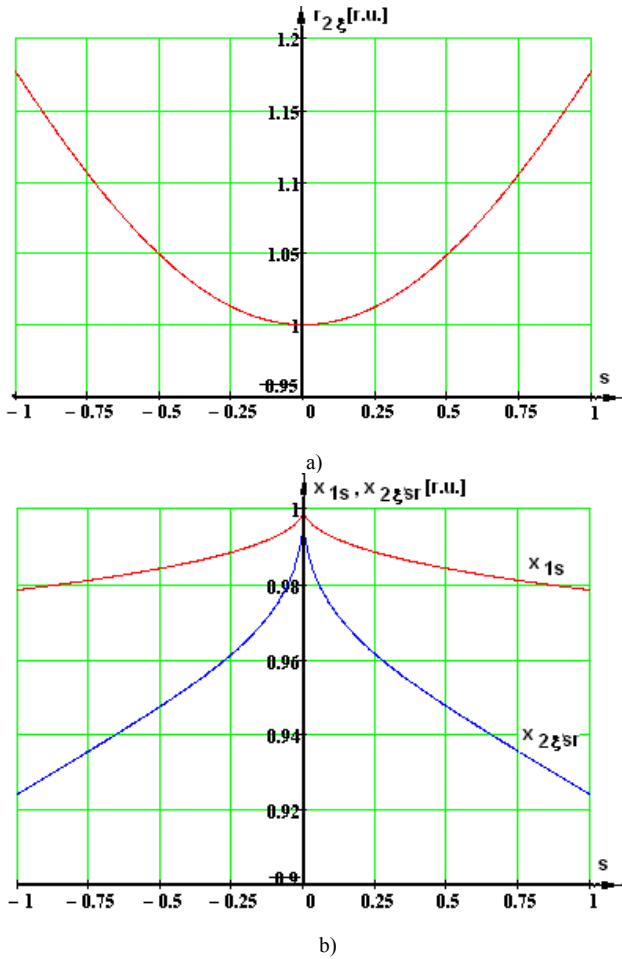


Fig. 4. a) The influence of the current repression over the resistance of the rotor winding; b) the dependency of the leakage reactances  $x_{1s}/x_{2s}$  – stator/ rotor by the slip (rotor with repression and saturation for the stator and the rotor).

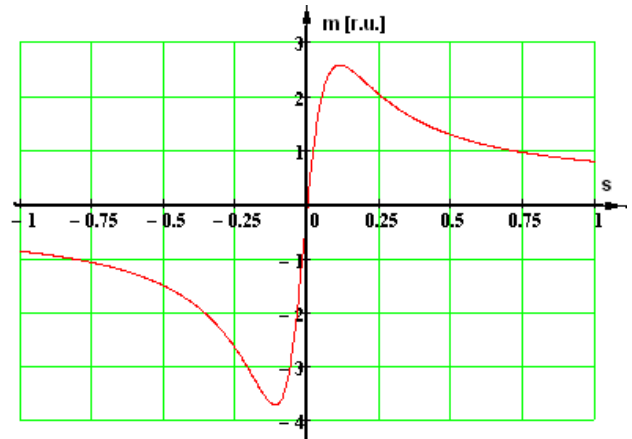


Fig. 5. Caracteristica mecanica naturala a motorului asincron.

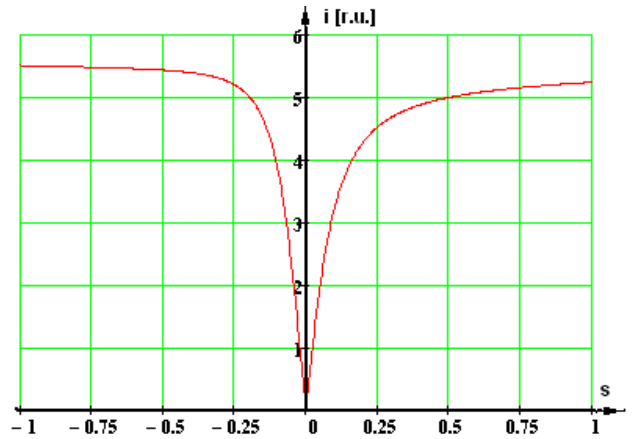


Fig. 6. Current characteristic for all the machine operating modes.

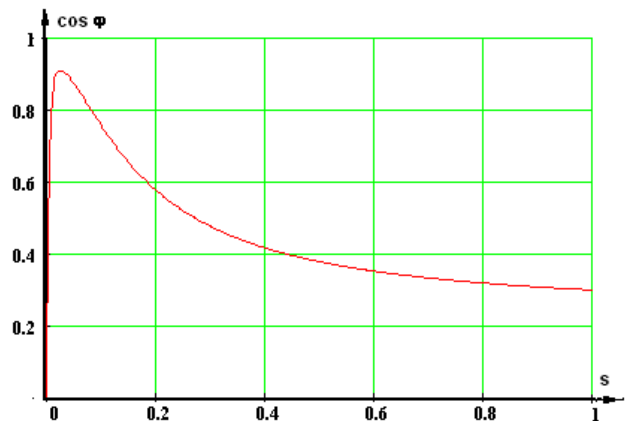


Fig. 7. Characteristic of the power factor during startup for the asynchronous motor

Considering during startup a parabolic variation curve of the current (the way of obtaining it being previously described), the variation of the windings leakage reactances ( $x_{1s}$  -stator and  $x_{2s}$  -rotor) with the magnetic saturation is obtained (Fig. 4.b).

With the values of these variable parameters (Fig. 4) the curves for the electromagnetic torque (Fig. 5), current (Fig. 6) and power factor (Fig. 7) were calculated and plotted for the generator and asynchronous motor operating modes.

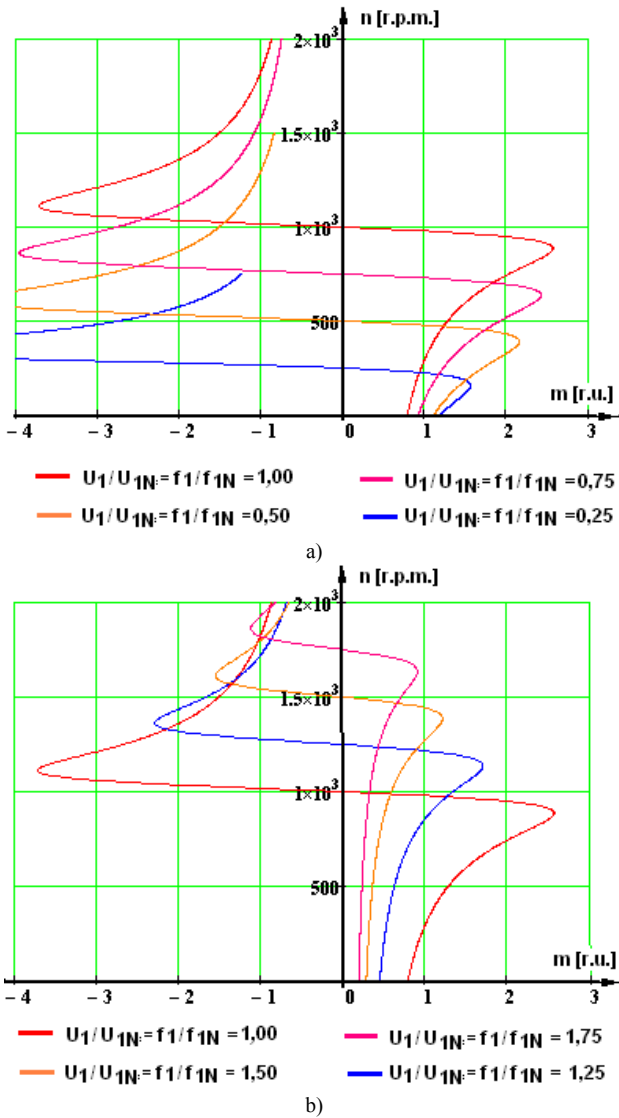


Fig. 8. The mechanical characteristics of the analyzed asynchronous motor:: a) when the ratio  $U_1/U_{1N}=f_1/f_{1N}$  is constant; b) for  $U_1=U_{1N}=\text{const}$  and  $f_{1N}<f_1$  variable.

The following is a study on the simulation of mechanical characteristics in the case when  $U_1/f_1=\text{const}$ . (constant torque operation) - Fig. 8.a, and for the case when  $U_1=\text{const}$  and  $f_1=\text{variable}$  - Fig. 8.b, respectively.

In Table I are depicted the results for the rated operating conditions obtained through simulation, and also the results known from the asynchronous motor datasheet. It is found that the values are very similar.

If the range of the variable  $i=1, 2, 3, \dots, 2 \cdot N/40$  is modified and the presented mathematical model is redone, for the motor slip the range  $s \in [-2.5, +2.5]$  results, corresponding to the stable operating modes as a motor or as a generator.

TABLE I. Results for the motor operating under rated conditions

Quantity analyzed	Symbol	MU	Results for the rated mode		
			Simulated	Datasheet	Error
Supply voltage	$U_{IN}$	V	1500	1500	-
Phase stator current	$I_{IN}$	A	121.4	119.6	1.51%
Speed	$n_N$	rpm	979.1	962.1	1.73%
Active power received from the supply network	$P_{IN}$	kW	283.8	289.5	2.01%

Apparent power received	$S_{IN}$	kVA	315.4	321.2	1.85%
Reactive power received from the supply network	$Q_{IN}$	kVAR	137.6	140.0	1.75%
Power factor	$\cos\phi_{IN}$		0.8997	0.914	1.61%
Efficiency	$\eta_N$		0.916	0.922	0.61%
Maximum torque	$m_m$		2.477	2.426	2.05%
Mass	$m$	kg	1180	1167	1.12%

CONCLUSIONS

The analysis of the results presented proves that, for the motor running under rated conditions, the deviations between the calculated values and the values provided in the datasheet are very low, under 2.1 %. This result validates the quality of the simulations performed, proving that the mathematical model is correct.

In the design process of the current asynchronous traction motors, the simulation of the mechanical or operating characteristics and the computation of the corresponding charactersitics, respectively, is a mandatory stage.

On this basis, the electromagnetic stresses and the constructive solutions can be definitively established, so that the machine corresponds in operation.

ACKNOWLEDGMENT

This work was supported by the grant POCU380/6/13/123990, co-financed by the European Social Fund within the Sectorial Operational Program Human Capital 2014 – 2020.

Contribution of authors:

First author – 50%

First coauthor – 20%

Second coauthor – 15%

Third coauthor – 15%

Received on November 20, 2019

Editorial Approval on November 29, 2019

REFERENCES

- [1] G. Popa, *Tracțiunea feroviară cu Motoare Asincrone trifazate*, Editura Matrix Rom, București, 2005.
- [2] A.D. Nicola, D.C. Cismaru, „Torque Equation and Torque-Speed Characteristics of traction Induction Motor”, *Proc. of OPTIM, Braşov*,1996.
- [3] D. Mihăilescu, *Locomotive și trenuri electrice cu motoare de tracțiune asincrone*, Editura Didactică și Pedagogică, București, 1997.
- [4] H. Toliat, “Recent Advances and Applications of Power Electronics and Motor Drives-Electric Machines and Motor Drives”, *Proc. of IECON, 2008*.
- [5] B. Fabrini, I. Boldea, ”Electric Machinery and Adjustable Speed Motor Drives. Part I-Guest Editorial”, *IEEE Trans. Ind. Electronics*, 54, 5, pp 2363-2364, 2007.
- [6] I. Boldea, S. Nasar, *The Induction Machine Handbook*, CRC Press, LLC USA, 2002.
- [7] J. W. Finch, D. Gsaoris, ”Contolled AC Electrical Drives”, *IEEE Trans. Ind. Electronics*, 55, 2,pp 481-491, 2008.
- [8] C. Iliăș, V. Bostan, *Utilizarea procesoarelor DSP în comanda numerică a motoarelor asincrone*, Editura Matrix Rom, București, 2005.
- [9] R. Krishnan, *Electric motor drives. Modeling, analysis and control*, Upper Saddle River, New Jersey, Prentice Hall, 2001.

- [10] V.I. Chrisanov, "Mathematical Model of the Induction Machines in Stator Reference Frame" (in Russian), *Electrotehnika*, Nr.7, 2004.
- [11] T. Dordea, G. Madescu, Il. Torac, M. Mot, L. Ocolisan, "Reducerea pierderilor în mașini electrice, sursă de energie utilizabilă", *Conferința Națională de Surse Noi și Regenerabile de Energie „CNSNRE 2003”*, Târgoviște 11-14 Septembrie 2003, 5 pag. (pe CD),
- [12] I. Vlad, A. Campeanu, S. Enache, *Computer-aided design of asynchronous motors. Optimization problems*, Universitaria Publishing House, Craiova, 2011 (in Romanian).